J. Adv. Model. Earth Syst., **Vol. 1**, Art. #10, 11 pp.

Single-layer axisymmetric model for a Hadley circulation with parameterized eddy momentum forcing

Adam H. Sobel[1] *and Tapio Schneider*[2]

[1] Department of Applied Physics and Applied Mathematics and Department of Earth and Environmental Sciences, Columbia University, New York, NY
[2] California Institute of Technology, Pasadena, CA

Manuscript submitted 26 May 2009; in final form 11 August 2009

An axisymmetric single-layer model is used to study interactions of the Hadley circulation with extratropical eddies. Eddy momentum fluxes are parameterized using a simple closure motivated by calculations with an idealized dry general circulation model (GCM). Calculations are performed in which the heating is parameterized as Newtonian relaxation of temperatures toward a prescribed radiative-convective equilibrium (RCE) state. The latitude at which the maximum RCE temperature occurs is varied to represent seasonal variations. In the axisymmetric model, as in the GCM, qualitative changes in the zonal momentum budget occur as the RCE temperature maximum moves away from the equator past a threshold latitude. For RCE temperature maxima closer to the equator, eddy momentum fluxes play a dominant role in the zonal momentum budget, nonlinearity is weak, and the meridional circulation is a weak function of the degree of asymmetry about the equator. For RCE temperature maxima sufficiently far from the equator, the zonal momentum budget becomes more nonlinear, angular momentum is more nearly conserved, and the circulation is a stronger function of the degree of asymmetry about the equator. Since the axisymmetric model can capture this behavior while being much simpler than the GCM, it may be a useful step towards a more comprehensive theory of the zonal-mean general circulation.

DOI:10.3894/JAMES.2009.1.10

1. Introduction

In idealized models, including several idealized general circulation models (Schneider 1984, Becker et al. 1997, Kim and Lee 2001, Walker and Schneider 2006, Schneider and Bordoni 2008, Bordoni and Schneider 2008), extratropical eddies have been shown to play an important role in determining the properties of the zonally averaged tropical overturning, or Hadley circulation. In these models, the eddies exert their influence most importantly through the zonal momentum budget, through a zonal-mean torque (eddy momentum flux divergence) in the upper troposphere. Observations are consistent with this picture in that they show that eddies are important in the tropical zonal momentum budget (Dima et al. 2005; Walker and Schneider 2006; Caballero 2007).

On the other hand, many studies have been performed with axisymmetric models in which the zonal-mean circulation is considered near-inviscid so that it approximately conserves angular momentum. Although the seminal studies that first developed these models did so with full recognition that, as was generally thought at the time, eddy effects might be important–e.g., presenting the inviscid axisymmetric models only as a starting point to provide a basic state for the consideration of eddy effects (Schneider and Lindzen 1977, Schneider 1977)–these models later seem to have been taken as providing a guide to the first-order dynamics of Earth's Hadley circulation, as suggested by the large number of studies examining the properties of the inviscid models (e.g., Held and Hou 1980, Lindzen and Hou 1988, Plumb and Hou 1992, Fang and Tung 1996, 1997, 1999, Polvani and Sobel 2002, Pauluis 2004, Burns et al. 2006, Boos and Emanuel 2008a,b), and the relatively small number directly considering eddy effects. Serious reconsideration of the notion that eddies are of first-order importance to the Hadley circulation is a relatively recent development. Full understanding of this idea and its implications requires further investigation. In this study, we present results from a single-layer axisymmetric model, which is able to capture qualitative aspects of the behavior of the Hadley circulation found in GCM simulations.

In GCM simulations and in observations of Earth's atmosphere, the degree to which eddies influence the Hadley circulation varies with season (Walker and

To whom correspondence should be addressed.
Adam Sobel, Columbia University, Dept. of Applied Physics and Applied Mathematics, 500 W. 120th St., Rm. 217, New York, NY 10027 USA
ahs129@columbia.edu

Table 1. Default model parameter values; different values are used in some calculations as stated in the text.

Parameter	Value	Definition
τ	37 d	Thermal relaxation time
H	16 km	Tropopause height
δ	4 km	Depth of layers in which meridional flow occurs
T_0	300 K	Reference temperature
Δ_z	60 K	Vertical potential temperature stratification
Δ_y	50 K	RCE equator-pole temperature gradient
θ_{00}	330 K	Background tropospheric-mean potential temperature
ϵ_u	10^{-8} s^{-1}	Background Rayleigh drag
ν_d	2.5 m s^{-1}	Parameterized eddy momentum flux coefficient
k_ν	7786 m^2/s	Diffusivity on v
β	2×10^{-11}m^{-1} s^{-1}	Meridional gradient of Coriolis parameter

Schneider 2006; Schneider and Bordoni 2008; Bordoni and Schneider 2008). For example, in the dry GCM simulations of Schneider and Bordoni (2008), diabatic heating is represented as Newtonian relaxation of temperatures toward an imposed axisymmetric radiative-equilibrium temperature profile (similarly as in many inviscid axisymmetric studies). At a given vertical level and given time, the equilibrium temperature profile has a single maximum and decreases with latitude away from that. A maximum at the equator corresponds to equinoctial conditions, in which the model solutions feature two tropical meridional overturning cells of comparable strength, one in each hemisphere. A maximum well off the equator corresponds to solstitial or monsoon conditions, in which the solutions feature one dominant tropical circulation cell, with ascent in the summer hemisphere and descent in the winter hemisphere. A seasonal cycle is imposed by smoothly varying the equilibrium temperature between these extremes. In the course of the seasonal cycle, the GCM's Hadley circulation undergoes sharp transitions from being strongly influenced by eddies in the equinoctial regime to being relatively weakly influenced by eddies (and thus bearing a greater correspondence to the classical inviscid theory) in the solstitial regime. Schneider and Bordoni (2008) and Bordoni and Schneider (2008) discuss the dynamics of these transitions and suggest that they may explain the observed rapid onset of the monsoons in Earth's atmosphere. As these transitions represent one of the more interesting features of the GCM results, and one absent from inviscid theory, capturing them in our simple model is a primary goal of the present study.

2. Model

a. Equations of motion

We use a model formulation adapted from Xian and Miller (2008). The model equations are

$$\partial_t u - v(\beta y - \partial_y u) = -\mathcal{H}(\partial_y v)(\partial_y v)u - \mathcal{F} - \mathcal{S}, \quad (2.1)$$

$$2(\partial_t v + v\partial_y v) + \beta y u = -\frac{gH}{T_0}\partial_y T + k_\nu \frac{\partial^2 v}{\partial y^2}, \quad (2.2)$$

$$\partial_t \theta + \frac{\delta \Delta_z}{H}\partial_y v = \frac{\theta_E - \theta}{\tau}. \quad (2.3)$$

The dynamical variables are taken to represent the flow in a thin layer of constant thickness δ adjacent to the tropopause at constant height H. The dynamical variables are the zonal and meridional velocities, u and v, and the temperature and potential temperature T and θ, related by

$$T = \theta(p_t/p_s)^{R/c_p}.$$

Here, p_s and p_t are fixed surface and tropopause pressures, and all other parameters are likewise taken to be fixed: the potential temperature difference Δ_z between the surface and tropopause (a static stability measure), the reference surface temperature T_0, and the thermal relaxation time τ. The radiative-convective equilibrium (RCE) temperature $\theta_E = \theta_E(y)$ is a prescribed function of latitude y, and $\mathcal{H}$ is the Heaviside function; $\mathcal{F}$ represents frictional drag and $\mathcal{S}$ eddy momentum flux divergence (EMFD), both of which we will parameterize in terms of the dynamical variables. Other notation is standard.

Xian and Miller (2008) present a derivation of a similar model, and Held and Phillips (1990) discuss another very similar model. The derivation starts from the primitive equations in the Boussinesq approximation; similar results can be obtained without the Boussinesq approximation by working in pressure coordinates, the difference being only in the interpretation of the fixed parameters. We assume that the meridional velocity vanishes outside the thin layer adjacent to the tropopause and outside a boundary layer adjacent to the surface. The Xian-Miller model (and ours) also includes vertical momentum advection, following earlier studies (Esler et al. 2000; Shell and Held 2004; Adam and Paldor 2009). In our case, vertical momentum advection is based on the assumption that mass injected into the upper layer carries a zonal velocity of zero. This is a simple and probably extreme assumption. We have repeated all key calculations with the opposite extreme assumption, that the mass injected into the upper layer carries the zonal velocity of the upper layer, which results in the elimination of the first term on the RHS of (2.1). The sensitivity of the results to this assumption is discussed below. If neither of these assumptions is made, one needs to explicitly model the velocity in the lower layer, as this velocity would appear in the vertical advection term; this may be a desirable model extension but we do not attempt it here. In deriving the meridional momentum equation, we also assume that the zonal velocity at the

lower boundary is much smaller than that near the tropopause.

The main differences between our model and that of Xian and Miller are as follows. Our zonal momentum equation represents only an integral over the thin upper layer in which the meridional velocity is nonzero, as opposed to the entire free troposphere; this eliminates coefficients involving the layer thickness in the zonal momentum equation. In both our model and Xian and Miller's, equation (2.2) results from integrating over the entire troposphere, which leads to the factor of two in the first term on the left-hand side (because of the assumptions that the meridional velocities at the surface and tropopause are equal and opposite, and that the surface zonal velocity is negligible compared to the tropopause zonal velocity). We retain nonlinear advection in this equation, whereas Xian and Miller do not (though this makes very little difference in the solutions). Also, we use a Newtonian relaxation of temperatures toward a prescribed RCE state, rather than their moist physics. Finally, we work on the equatorial β-plane rather than the sphere.

We include a Rayleigh drag term

$$\mathcal{F} = \epsilon_u u \tag{2.4}$$

with a (typically small) coefficient ϵ_u in the zonal momentum equation to ensure the axisymmetric model has a stable steady state, although this drag has no clear physical analog in the atmosphere. We parameterize the eddy momentum flux divergence as

$$\mathcal{S} = v_d \mathcal{H}(u)\mathrm{sgn}(y)\partial_y u \tag{2.5}$$

with a constant drag velocity v_d. The Heaviside function represents the fact that the energy-containing extratropical eddies with westerly (or zero) phase speeds, which originate in regions of westerly flow and propagate toward the tropics, reach their critical latitudes and dissipate or are reflected before they can propagate into regions of easterly flow. This parameterization is empirical, motivated by the eddy momentum flux divergence in the idealized GCM integrations of Schneider and Bordoni (2008). It gives a total EMFD integrated over a Hadley cell that is proportional to the zonal wind u at the subtropical terminus of the cell and thus, by thermal wind balance, scales with the meridional temperature gradient there. This is roughly, although not quantitatively, consistent with the scaling of the integrated EMFD in simulations of a wide range of climates with an idealized dry GCM (Schneider and Walker (2008): in those simulations, the integrated EMFD depends roughly on the square root of the extratropical meridional temperature gradient if baroclinic eddies are sufficiently strong.).

Figure 1 shows the eddy momentum flux divergence in those simulations, together with that computed using (2.5) and the zonal mean zonal winds from the same simulations, with $v_d = 2.5$ m s^{-1}. In both cases, the GCM output is averaged between the vertical levels in sigma coordinates $0.15 < \sigma < 0.35$ (corresponding approximately to pressures between 150 and 350 hPa). The simulations use thermal forcing whose maximum is offset by a distance y_0 from the equator (see Schneider and Bordoni's equation (2), or equation (3.2) below), shown on the vertical axis of the plots, while meridional distance y is shown on the horizontal axis. There are sizable discrepancies between the GCM output and the parameterized EMFD, particularly outside the Hadley cells and in the summer hemisphere. But the parameterization captures the qualitative behavior of the EMFD in the winter subtropics, which is of primary interest here as it affects the strong cross-equatorial Hadley cell.

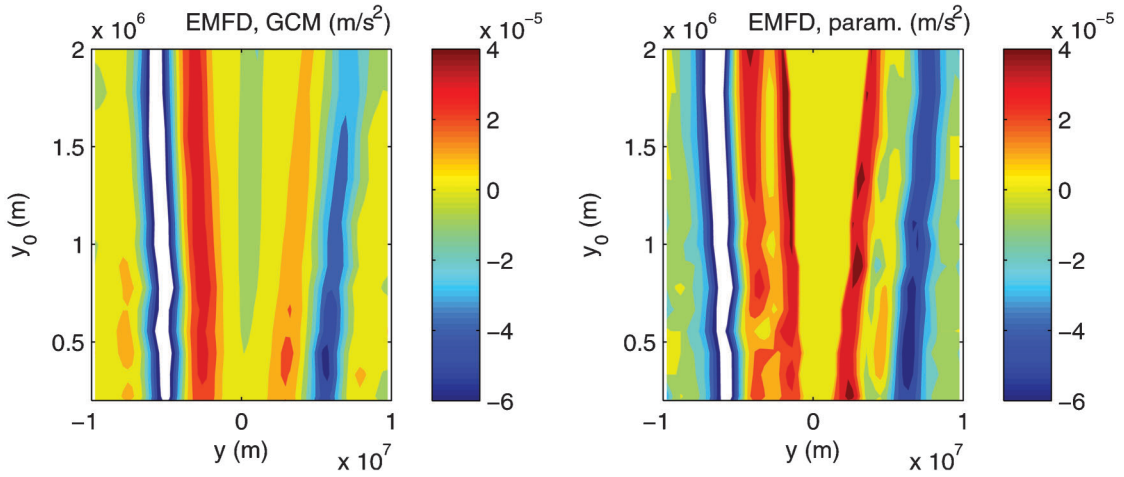

Fig. 1. Top: eddy momentum flux divergence (m s^{-2}) from the GCM simulations of Schneider and Bordoni (2008), plotted as a function of thermal forcing asymmetry, y_0 and meridional distance, y. Bottom: eddy momentum flux divergence computed using the parameterization in equation (2.5) and the zonal mean zonal winds from the same simulation used in the top panel, with drag velocity $v_d = 2.5$ m s^{-1}. The white color refers to negative values smaller than -6×10^{-5} m s^{-2}.

b. Numerical solution

Our numerical code solves (2.1)–(2.3) on a staggered grid, using a leapfrog time stepping scheme and a first-order upwind finite difference scheme for the advection terms. We use a domain of meridional half-width 15751 km with 801 gridpoints for v and 800 gridpoints for u and θ, for a resolution of 39.3 km. We require that $v = 0$ at the lateral boundaries. This renders the equations for u and θ singular there; however, in practice our forcing is such that u and v are both zero and θ is constant over a large region adjacent to each lateral boundary, so that the boundary conditions are unimportant.

The diffusivity on v, shown on the RHS of (2.2), is taken to be small ($k_v = 7786$ m^2 s^{-1}), and is included to reduce numerical noise. Very small fluctuations in the instantaneous meridional velocity field remain; these are too small to see in plots except for the weakest circulations, such as that shown in Fig. 2, in which a very small scale is used for the v-axis. In that figure, more noise would be visible if we had plotted the instantaneous meridional velocity field. Averaging in time as in Fig. 2 suffices to largely eliminate the fluctuations. For cases with stronger circulations, time averaging is not needed to produce plots in which the noise is too small to be visible.

3. Results

a. Comparison with analytical solutions

We first consider a near-inviscid case, in which an analytical solution is possible (see the appendix) and can be used to

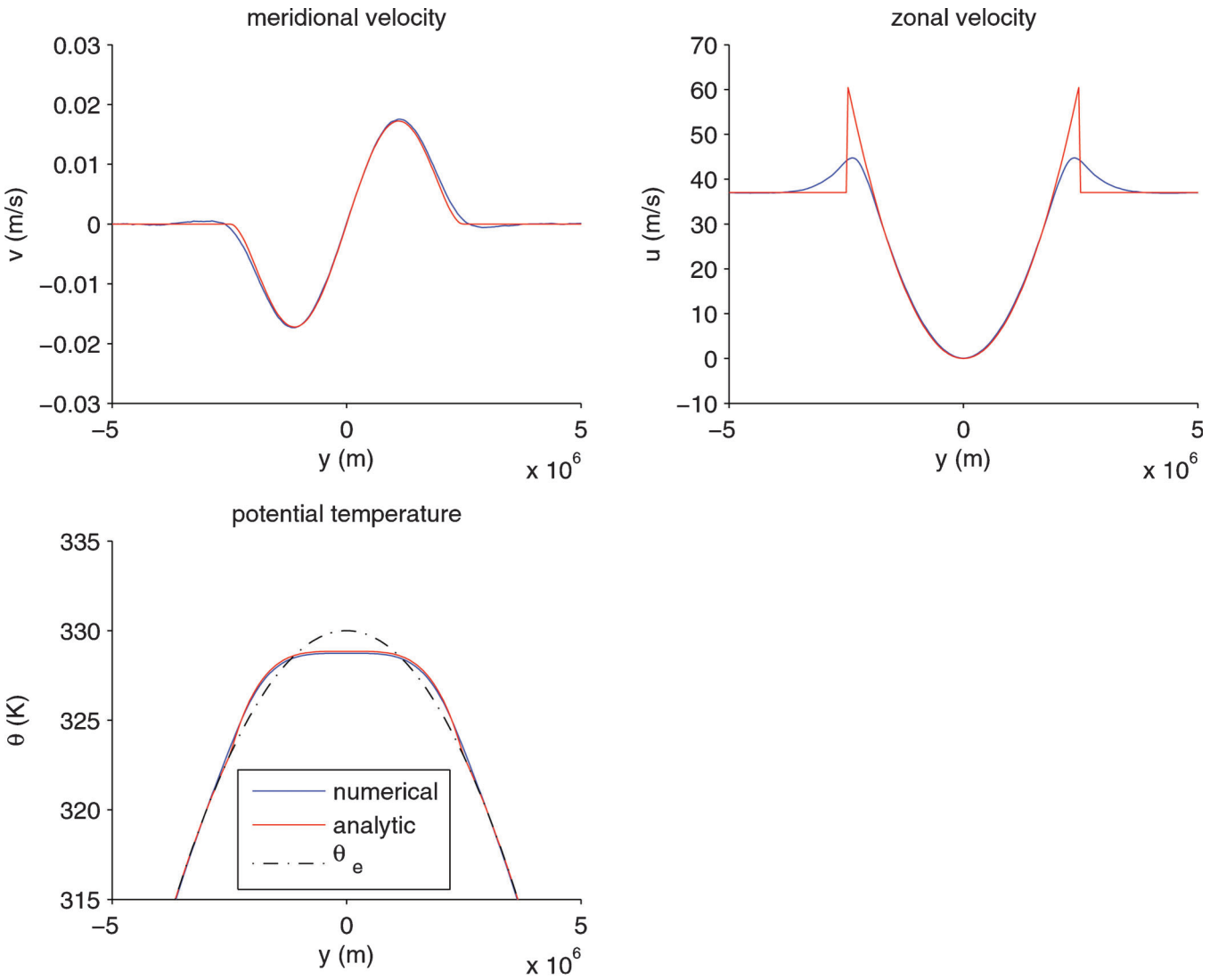

Fig. 2. Analytical vs. numerical solutions with no imposed EMFD, no vertical momentum advection, and Rayleigh drag coefficient equal to 10^{-10} s^{-1}. Numerical solutions are in blue and analytical in red; in the lower left panel, the radiative-convective equilibrium profile θ_E is also shown by the dot-dash curve.

test the numerical code. We consider a case in which there is no eddy momentum flux divergence ($\mathcal{S}=0$), ϵ_u is very small, and the thermal forcing is

$$\theta_E = \begin{cases} \theta_{00} - \Delta_y \left(\dfrac{y}{y_1}\right)^2 & \text{for } |y| < y_1, \\ \theta_{00} - \Delta_y & \text{for } |y| \geq y_1. \end{cases} \tag{3.1}$$

In addition, for the sake of analytical tractability, we neglect the vertical advection term in the zonal momentum equation (the first term on the RHS of (2.1)). The forcing parameters are $\theta_{00} = 330$ K, $\Delta_y = 100$ K, $\Delta_z = 60$ K, $y_1 = 9439$ km. The dynamical parameters are $H = 16$ km, $T_0 = 300$ K, and $\beta = 2 \times 10^{-11}$ m^{-1} s^{-1}.

Figure 2 shows a comparison between the numerical solution and the analytical solution presented in the appendix. The agreement is very good, giving us confidence in our numerical code.

b. Sensitivity to Rayleigh drag

In this section, we present the sensitivity of our axisymmetric solutions to the Rayleigh drag coefficient ϵ_u, with no EMFD ($\mathcal{S}=0$). This is of interest in its own right, but also necessary for a proper understanding of our results with $\mathcal{S}\neq 0$. When the θ_E maximum is a significant distance from the equator, it will turn out that we need a somewhat larger value of ϵ_u than that for which the solution converges to the inviscid analytical one for the hemispherically symmetric forcing (the only case for which we have computed the analytical solution). We need to understand how this larger value of ϵ_u influences the solution.

Figure 3 shows results from calculations using the same forcing as used for Fig. 2, but with three different values of ϵ_u: the smallest is 10^{-9} s^{-1}, a factor of 10 greater than that used in Fig. 2, while the other two are larger by factors of 10 and 100, respectively. Results for $\epsilon_u = 10^{-10}$ s^{-1}, (not shown) are indistinguishable from those for $\epsilon_u = 10^{-9}$ s^{-1}, within the thickness of the lines on the plots. The maximum value of v is 50% larger than that for the near-inviscid solution when $\epsilon_u = 10^{-8}$ s^{-1}, and much larger when $\epsilon_u = 10^{-7}$ s^{-1}. This is expected since in steady state, the Rayleigh drag can only be balanced by advection of angular momentum, requiring meridional flow. In the linear regime, in which only planetary angular momentum is advected, the balance in (2.1) is $\beta y v \sim \mathcal{F}$, which is known in the stratospheric literature as "downward control" (Haynes et al. 1991). The solutions of interest here are nonlinear, so that in steady state $v(\beta y - \partial_y u) \sim \mathcal{F}$, but it is still the case that v increases with $\mathcal{F}$, at least for hemispherically symmetric thermal forcing (with asymmetric thermal forcing, v may decrease with $\mathcal{F}$ because the zonal flow may weaken with increasing $\mathcal{F}$ (Walker and Schneider 2005)). In fact, the dependence is stronger in the nonlinear regime than in the linear, because the absolute vorticity $\beta y - \partial_y u$ is invariably smaller than the planetary component βy alone; in inviscid theory, the absolute vorticity vanishes within the Hadley cell.

Next we present calculations evaluating the sensitivity to ϵ_u using the model configuration which we will use for the rest of the study. We now include the vertical advection term in (2.1) and specify the thermal forcing, following Schneider and Bordoni (2008), as

$$\theta_E = \theta_{00} - \Delta_y \left[\sin^2\left(\frac{\pi y}{2y_1}\right) + 2\sin\left(\frac{\pi y_0}{2y_1}\right)\sin\left(\frac{\pi y}{2y_1}\right)\right]. \tag{3.2}$$

Here, θ_{00} and y_1 are as above, but we set $\Delta_y = 50$ K. Figure 4 shows results for equatorially symmetric forcing, $y_0 = 0$, and the same three values of ϵ_u used for Fig. 3.

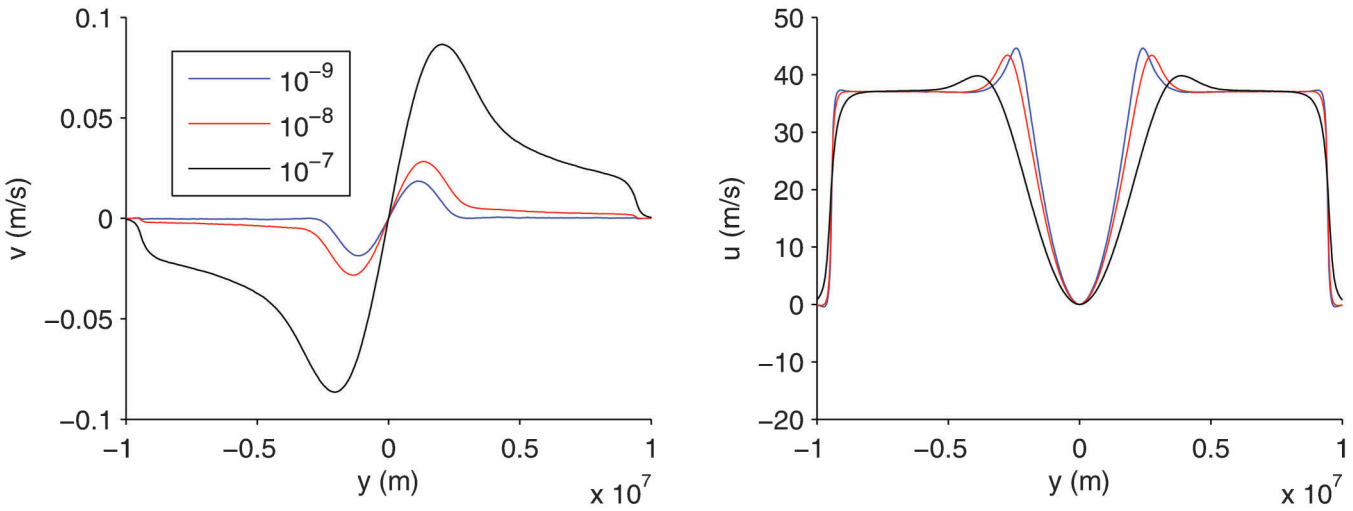

Fig. 3. Numerical solutions for meridional velocity (left) and zonal velocity (right) with no imposed EMFD ($\mathcal{S}=0$), no vertical momentum advection, the same forcing as in Fig. 2, and Rayleigh drag coefficient ϵ_u equal to 10^{-9} s^{-1} (blue), 10^{-8} s^{-1} (red), and 10^{-7} s^{-1} (black). Results for $\epsilon_u = 10^{-10}$ s^{-1} (not shown) are indistinguishable from those for $\epsilon_u = 10^{-9}$ s^{-1}, within the thickness of the curves.

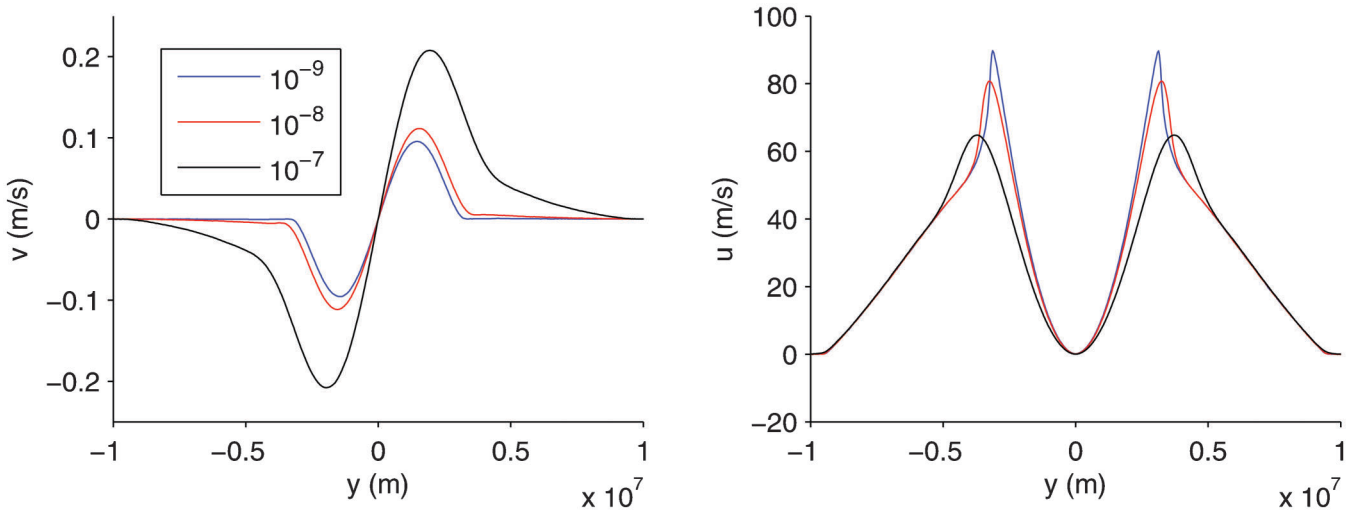

Fig. 4. As in Fig. 3, but with thermal forcing as in (3.2) with $y_0 = 0$, and vertical advection of zonal momentum included.

Comparing Figs. 3 and 4, we see that when the circulation is stronger, the percentagewise impact of small Rayleigh drag is smaller. The maximum value of v is now only 16% larger when $\epsilon_u = 10^{-8}$ s^{-1} than that for the near-inviscid solution ($\epsilon_u = 10^{-9}$ s^{-1}); it is about twice as large when $\epsilon_u = 10^{-7}$ s^{-1}. This is further supported by Fig. 5, which shows results from a set of calculations identical to those in Fig. 4, except that the thermal forcing is centered well off the equator, $y_0 = 1000$ km. The results feature a very strong winter subtropical jet and relatively weak summer jet, and a single-celled meridional circulation for all but the largest value of ϵ_u shown. It is now only for this largest value, 10^{-7} s^{-1} (corresponding to a damping timescale of 116 days), that the meridional circulation departs significantly (20%) from that of the less dissipative solutions.

c. Calculations with varying off-equatorial forcing

Figure 6 presents results from a set of calculations in which y_0 is varied from 0 to 2000 km in intervals of 200 km. Each calculation is carried out until a steady state is reached. The zonal and meridional velocity fields in the steady state are contoured as functions of y and y_0; any horizontal cut gives u or v as a function of y from a single calculation with a given y_0. As y_0 increases, the winter jet strengthens and moves poleward, the summer jet weakens, and the equatorial easterlies strengthen, while the meridional circulation also strengthens. These qualitative features are familiar from previous work (e.g., Lindzen and Hou 1988).

The region in which the local Rossby number $\mathrm{Ro} = -\zeta/(\beta y) > 0.6$, where $\zeta = -\partial u/\partial y$ is the relative vorticity, is indicated by the heavy black contours. We see that the

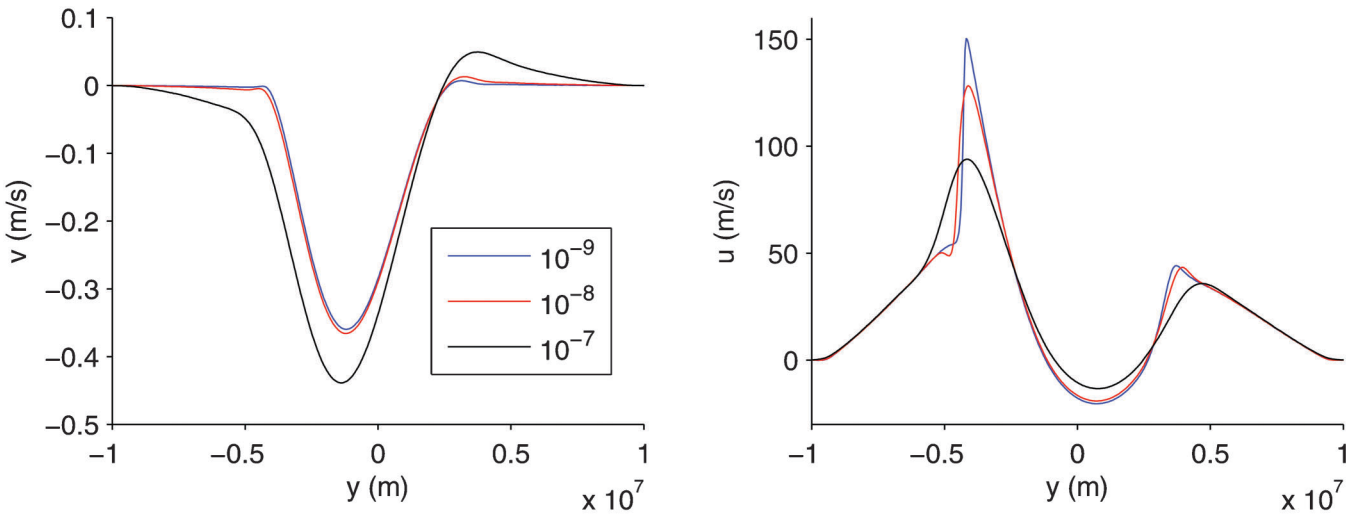

Fig. 5. As in Fig. 4, but with $y_0 = 1000$ km.

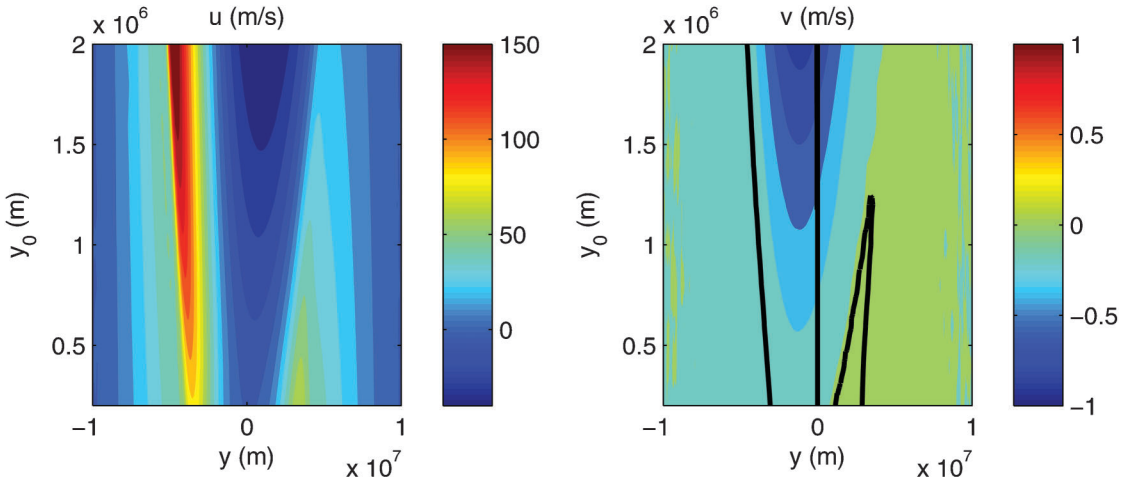

Fig. 6. Plots of (left) zonal velocity, u (m s^{-1}), and (right) meridional velocity, v (m s^{-1}), as a function of latitudinal position, y, on the horizontal axis and of the θ_E maximum, y_0, on the vertical axis. In the plot of v, heavy black contours enclose regions of Ro $= -\zeta/(\beta y) > 0.6$.

maximum absolute value of v lies within the region where Ro > 0.6 for all y_0. In a region of constant angular momentum, as occurs within the Hadley cell in near-inviscid theory, Ro $= 1$, while in the linear downward control regime, Ro $\ll 1$. Thus the region in which Ro > 0.6 roughly delineates the region in which the flow is reasonably close to conserving angular momentum. In these calculations with $\mathcal{S} = 0$ and small $\mathcal{F}$, this region encloses most of the region in which the meridional flow is significant, as expected.

d. Parameterized eddy momentum flux divergence

We present a set of calculations in which $\mathcal{S}$, the eddy momentum flux divergence due to baroclinic eddies, parameterized according to (2.5), is nonzero.

Figure 7 presents, in the top two panels, a set of calculations identical to that in Fig. 6, except that $\mathcal{S}$ is nonzero and parameterized according to (2.5), with $\nu_d = 2.5$ m s^{-1} as in Fig. 1 for the idealized GCM. The lower two panels show results from the idealized GCM (Schneider and Bordoni 2008), averaged over the vertical sigma levels $0.15 < \sigma < 0.35$ as in Fig. 1. In both cases, results are plotted as functions of meridional distance y and distance of the θ_E maximum from the equator y_0; recall, however, that the axisymmetric model is formulated on the β-plane while the GCM is on the sphere.

A broad qualitative resemblance between the results from the two models is apparent. At a finer level of detail a number of differences are evident, but some key qualitative features are nonetheless captured by the axisymmetric model.

Both the tropical easterlies and extratropical winter westerlies are stronger and have broader maxima in the axisymmetric model than in the GCM, particularly at large y_0. In the case of the westerlies, this may be in part due to the lack of eddy heat fluxes in the axisymmetric model, as these tend to reduce the meridional temperature gradient and thus also the winds in the subtropics. The summer westerly jet is stronger in the GCM than in the axisymmetric model at large y_0.

In the axisymmetric model, the maximum v (in absolute value) lies in a region of small local Rossby number when y_0 is small; in those cases, Ro > 0.6 only in a very small region near the equator. At larger y_0, the region in which Ro > 0.6 expands into the winter hemisphere, while simultaneously the location of the tropical peak in v moves equatorward, so that eventually the two overlap at large y_0. In the GCM, qualitatively similar results hold. The region in which Ro > 0.6 is smaller and the peak values of meridional velocity are smaller in the GCM; the location of peak meridional velocity moves equatorward more strongly in the GCM as y_0 increases.

The GCM has an extratropical equatorward-flowing Ferrel cell in the winter hemisphere, which the axisymmetric model largely lacks. This is explained by stronger eddy momentum flux divergence in the GCM, as can be seen by comparing Figs. 1 and 8, and also by the larger Coriolis parameter at high latitudes in the axisymmetric model, since it is on an equatorial β-plane as opposed to the spherical GCM, and at high latitudes v is determined by the linear balance $fv \approx \mathcal{S}$. This difference does not concern us, as we are interested in the tropical circulation here.

Figure 8 shows the eddy momentum flux divergence from the axisymmetric model, plotted as a function of y and y_0. There is broad qualitative agreement with the GCM results in Fig. 1, though the regions of strong positive EMFD in the axisymmetric model's winter hemisphere are broader, occur further poleward, and increase in magnitude more strongly as y_0 increases compared to the GCM. The negative EMFD at high latitudes is stronger in the GCM, particularly at small y_0.

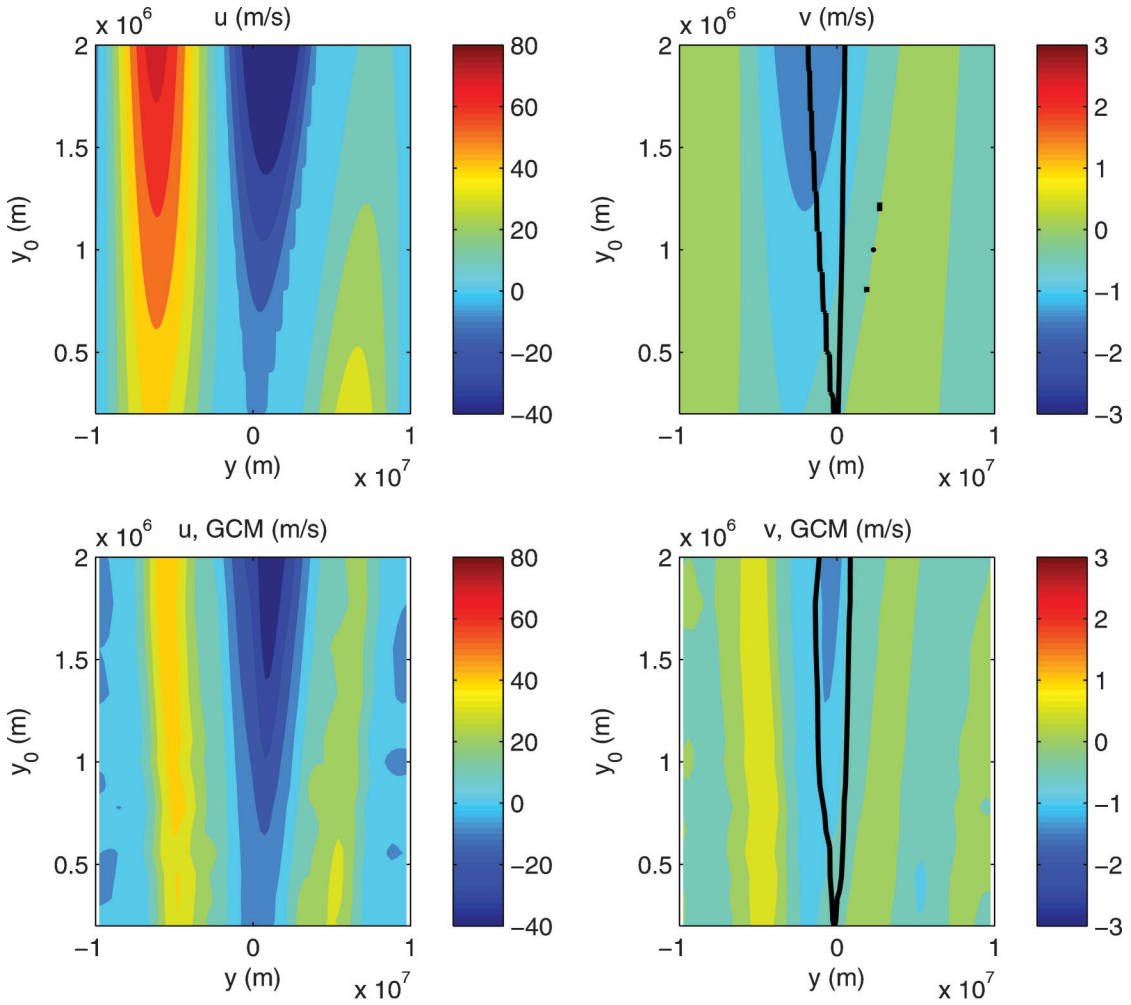

Fig. 7. As in Fig. 6, but for calculations with EMFD included. GCM results are shown on the bottom row.

Given the better agreement between the two panels of Fig. 1 than between the single-layer results shown here and either one of the former, the proximate cause of the disagreement is apparently the different zonal mean zonal winds in the two models, rather than the functional form of the parameterization (2.5) itself. However, the winds themselves are determined by strong feedbacks between the eddies (whether explicit or parameterized) and the mean flow, so it is quite possible that discrepancies which appear relatively small in comparisons such as that in Fig. 1 may lead to larger ones in interactive calculations such as that shown in Fig. 8. Despite these differences, the similarities are apparently strong enough to reproduce at least qualitatively, and to some degree quantitatively, key features of the GCM solutions, such as the transitions in the dynamics of the circulation as y_0 increases.

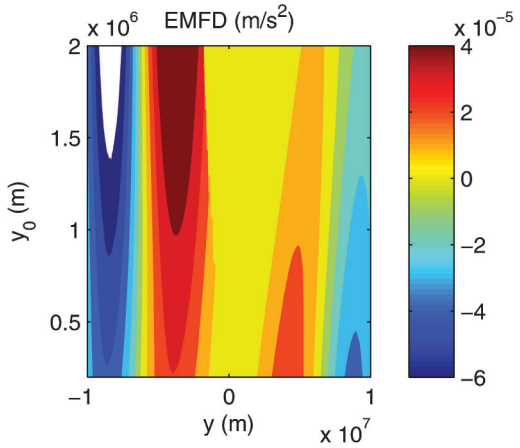

Fig. 8. Eddy momentum flux divergence (m s^{-2}) from the single-layer model. The white color refers to negative values less than 6×10^{-5} m s^{-2}.

Figure 9 displays the maximum absolute value of v as a function of y_0 from the axisymmetric model, both on logarithmic scales. This figure shows that the transition from a more linear to a more nonlinear zonal momentum budget described above corresponds approximately to a change between two different power laws, a shallower one for small y_0 and a steeper one for large y_0. Reference power laws of $y_0^{1/5}$ and $y_0^{3/4}$, those found to be a good fit to the

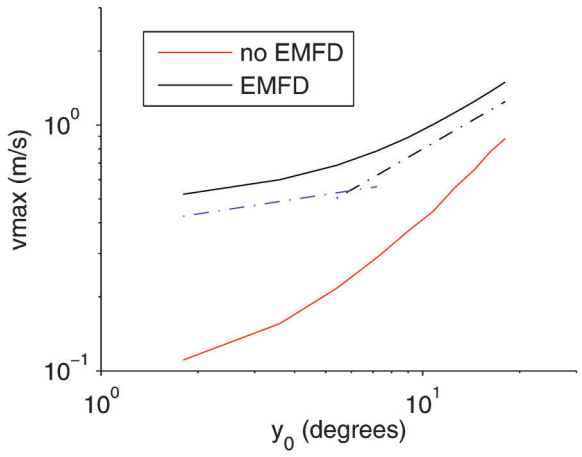

Fig. 9. Log-log plot of maximum meridional velocity as a function of y_0, for the calculations with eddy momentum flux divergence (black) and without (red). Reference power laws of $y_0^{1/5}$ and $y_0^{3/4}$ are shown by the blue and black dot-dash lines, respectively.

GCM results by Schneider and Bordoni (2008), are also shown on the figure. The axisymmetric model results with parameterized EMFD are close to these power laws. The calculations with $\mathcal{S}=0$, also shown in the figure, deviate from a pure single power law, but considerably less so. The difference in the maximum v between the two sets of calculations is maximal at the smallest value of y_0 shown and minimal at the largest, indicating that near-inviscid solutions are most relevant for larger y_0.

4. Conclusions

We have performed a set of calculations with an axisymmetric single-layer model in which parameterized eddy momentum fluxes are included. We first tested the underlying model without the eddy momentum flux parameterization to demonstrate that it could reproduce analytical results from classical near-inviscid theory and then that small amounts of background Rayleigh drag would not dramatically distort the solution. We then added the eddy momentum flux parameterization and compared the results both to the near-inviscid model and to the idealized GCM simulations of Bordoni and Schneider (2008).

The model with eddy momentum flux divergence is able to reproduce key qualitative features of the idealized GCM simulations. In particular, as the latitude of maximum thermal forcing is increased, there is a transition from a more linear regime, in which the maximum meridional velocity occurs in a region of small local Rossby number, to a more nonlinear one, more similar to that in near-inviscid theory, in which the maximum meridional velocity occurs in a region of larger local Rossby number.

These results suggest that the axisymmetric model may be a useful step towards a theory of the Hadley cell in which eddy effects are included. Lacking both longitudinal and vertical structure, the axisymmetric model reduces the problem to a one-dimensional one, rendering it relatively amenable to analysis. However, it still remains a difficult problem to understand the interaction between nonlinear momentum advection by the mean meridional circulation and eddy momentum flux divergence, both of which are important in Earth's Hadley circulation.

Acknowledgments: We are grateful for support by the National Science Foundation via grant nos. ATM-0450059 (TS) and ATM-0542736 (AHS) and a David and Lucile Packard Fellowship (TS).

Much of the work was done during the academic year 2007-2008 while the first author was a sabbatical visitor at the Centre for Australian Weather and Climate Research, Bureau of Meteorology, in Melbourne, Australia, and he thanks the scientists and administrative staff of that institution for their support and hospitality

We thank Paul O'Gorman for helpful discussion about and suggestions for the eddy momentum flux parameterization we used.

Appendix A: derivation of analytical solutions

We seek steady analytical solutions, and follow the standard recipe from inviscid Hadley circulation theory. We neglect all terms on the RHS of (2.1) and the advection and diffusion terms in (2.2)—although the Rayleigh friction term in (2.1) and both the advection and diffusion terms in (2.2) are retained in our numerical code—so that we are analyzing the steady state system

$$-v\left(\beta y-\frac{du}{dy}\right)=0, \tag{4.1}$$

$$\beta y u=-\frac{gH}{T_0}\frac{dT}{dy}, \tag{4.2}$$

$$\frac{\delta\Delta_z}{H}\frac{dv}{dy}=\frac{\theta_E-\theta}{\tau}. \tag{4.3}$$

As usual, we seek solutions in which there is a meridional circulation in some region near the equator ($|y| \le y_H$) and no meridional circulation and $\theta = \theta_E$ in a region away from the equator ($|y| > y_H$). We require that θ be continuous at $y = y_H$, the boundary between the two regions. In the region of non-vanishing meridional circulation ($v \neq 0$), we can divide (4.1) by v and integrate to find that the zonal velocity must satisfy

$$u=\frac{1}{2}\beta y^2+c_1. \tag{4.4}$$

The constant c_1 is determined by requiring that the limit as $\epsilon_u \to 0$ not be singular. In that limit symmetry shows that

there is no term which can balance the Rayleigh drag, however small, on a finite zonal velocity at $y = 0$. Thus $c_1 = 0$ and

$$u = \frac{1}{2}\beta y^2. \tag{4.5}$$

Using (3.1) and assuming $|y_H| < y_1$, we integrate (4.2) and require that $\theta = \theta_E$ at $y = y_H$, leading to

$$\theta = \theta_{00} - \Delta_y \left(\frac{y_H}{y_1}\right)^2 + D\left(y_H^4 - y^4\right), \tag{4.6}$$

where

$$D = \frac{1}{8}\frac{T_0}{L_R^4}\left(\frac{p_s}{p_t}\right)^{R/c_p}$$

with equatorial Rossby radius $L_R = \left(\sqrt{gH}\Big/\beta\right)^{1/2}$.

Integrating (4.3) and using (4.6) yields the solution for v,

$$v = \frac{H}{\delta\Delta_z\tau}\left[\frac{\Delta y}{y_1^2}\left(y_H^2 y - \frac{y^3}{3}\right) + D\left(\frac{y^5}{5} - y_H^4 y\right)\right], \tag{4.7}$$

where the integration constant has been set to zero since symmetry requires $v = 0$ at the equator. The Hadley cell boundary y_H is still unknown at this point, but it is found by requiring that v be continuous at y_H, and thus zero there. The result is

$$y_H = \left(\frac{5\Delta_y}{6y_1^2 D}\right)^{1/2}. \tag{4.8}$$

This expression for the Hadley cell boundary has the same dependence on parameters such as β and Δ_y as the classic solution of Held and Hou's (1980) model, as it should given the similarity of the models and of the functional forms of the thermal forcings.

References

Adam, O., and N. Paldor, 2009: Global circulation in an axially symmetric shallow water model forced by equinoctial differential heating. *J. Atmos. Sci.*, **66**, 1418–1433, doi: 10.1175/2008JAS2685.1.

Becker, E., G. Schmitz, and R. Geprags, 1997: The feedback of midlatitude waves onto the Hadley cell in a simple general circulation model. *Tellus*, **49A**, 182–199, doi: 10.1034/j.1600-0870.1997.t01-1-00003.x.

Boos, W. R., and K. A. Emanuel, 2008a: Wind-evaporation feedback and abrupt seasonal transitions of weak, axisymmetric Hadley circulations. *J. Atmos. Sci.*, **65**, 2194–2214, doi: 10.1175/2007JAS2608.1.

Boos, W. R., and K. A. Emanuel, 2008b: Wind-evaporation feedback and the axisymmetric transition to angular momentum conserving Hadley flow. *J. Atmos. Sci.*, **65**, 3758–37781, doi: 10.1175/2008JAS2791.1.

Bordoni, S., and T. Schneider, 2008: Monsoons as eddy-mediated regime transitions of the tropical overturning circulation. *Nature Geosci.*, **1**, 515–519, doi: 10.1038/ngeo248.

Burns, S. P., A. H. Sobel, and L. M. Polvani, 2006: Asymptotic solutions to the moist axisymmetric Hadley circulation. *Theor. Comp. Fluid Dyn.*, **20**, 443–467, doi: 10.1007/s00162-006-0024-z.

Caballero, R., 2007: Role of edddies in the interannual variability of Hadley cell strength. *Geophys. Res. Lett.*, **34**, L22705, doi: 10.1029/2007GL030971

Dima, I., J. M. Wallace, and I. Kraucunas, 2005: Tropical zonal momentum balance in the NCEP reanalyses. *J. Atmos. Sci.*, **62**, 2499–2513, doi: 10.1175/JAS3486.1.

Esler, J. G., L. M. Polvani, and R. A. Plumb, 2000: The effect of the Hadley circulation on the propagation and reflection of planetary waves in a simple one-layer model. *J. Atmos. Sci.*, **57**, 1536–1556, doi: 10.1175/1520-0469(2000)057<1536:TEOAHC>2.0.CO;2.

Fang, M., and K. K. Tung, 1996: A simple model of nonlinear Hadley circulation with an ITCZ: analytic and numerical solutions. *J. Atmos. Sci.*, **53**, 1241–1261, doi: 10.1175/1520-0469(1996)053<1241:ASMONH>2.0.CO;2.

Fang, M., and K. K. Tung, 1997: The dependence of the Hadley circulation on the thermal relaxation time. *J. Atmos. Sci.*, **54**, 1379–1384, doi: 10.1175/1520-0469(1997)054<1379:TDOTHC>2.0.CO;2.

Fang, M., and K. K. Tung, 1999: Time-dependent nonlinear Hadley circulation. *J. Atmos. Sci.*, **56**, 1797–1807, doi: 10.1175/1520-0469(1999)056<1797:TDNHC>2.0.CO;2.

Haynes, P. H., M. E. McIntyre, T. G. Shepherd, C. J. Marks, and K. P. Shine, 1991: On the "downward control" of extratropical diabatic circulations by eddy-induced mean zonal forces. *J. Atmos. Sci.*, **48**, 651–6782, doi: 10.1175/1520-0469(1991)048<0651:OTCOED>2.0.CO;2.

Held, I. M., and A. Y. Hou, 1980: Nonlinear axially symmetric circulations in a nearly inviscid atmosphere. *J. Atmos. Sci.*, **37**, 515–533, doi: 10.1175/1520-0469(1980)037<0515:NASCIA>2.0.CO;2.

Held, I. M., and P. J. Phillips, 1990: A barotropic model of the interaction between the Hadley cell and a Rossby wave. *J. Atmos. Sci.*, **47**, 856–869, doi: 10.1175/1520-0469(1990)047<0856:ABMOTI>2.0.CO;2.

Kim, H., and S. Lee, 2001: Hadley cell dynamics in a primitive equation model. Part II: Nonaxisymmetric flow. *J. Atmos. Sci.*, **58**, 2859–2871, doi: 10.1175/1520-0469(2001)058<2859:HCDIAP>2.0.CO;2.

Lindzen, R. S., and A. Y. Hou, 1988: Hadley circulations for zonally averaged heating centered off the equator. *J. Atmos. Sci.*, **45**, 2416–2427, doi: 10.1175/1520-0469(1988)045<2416:HCFZAH>2.0.CO;2.

Pauluis, O., 2004: Axisymmetric circulation in a moist atmosphere. *J. Atmos. Sci.*, **61**, 1161–1173, doi: 10.1175/1520-0469(2004)061<1161:BLDACH>2.0.CO;2.

Plumb, R. A., and A. Hou, 1992: The response of a zonally-symmetric atmosphere to subtropical thermal forcing. *J. Atmos. Sci.*, **49**, 1790–1799, doi: 10.1175/1520-0469(1992)049<1790:TROAZS>2.0.CO;2.

Polvani, L. M., and A. H. Sobel, 2002: The Hadley circulation and the weak temperature gradient approximation. *J. Atmos. Sci.*, **59**, 1744–1752, doi: 10.1175/1520-0469(2002)059<1744:THCATW>2.0.CO;2.

Schneider, E. K., 1977: Axially symmetric steady-state models of the basic state for instability and climate studies. Part II. Nonlinear calculations. *J. Atmos. Sci.*, **34**, 280–296, doi: 10.1175/1520-0469(1977)034<0280:ASSSMO>2.0.CO;2.

Schneider, E. K., 1984: Response of the annual and zonal mean winds and temperatures to variations in the heat and momentum sources. *J. Atmos. Sci.*, **41**, 1093–1115, doi: 10.1175/1520-0469(1984)041<1093:ROTAAZ>2.0.CO;2.

Schneider, E. K., and R. S. Lindzen, 1977: Axially symmetric steady-state models of the basic state for instability and climate studies. Part I. Linearized calculations. *J. Atmos. Sci.*, **34**, 263–279, doi: 10.1175/1520-0469(1977)034<0263:ASSSMO>2.0.CO;2.

Schneider, T., and S. Bordoni, 2008: Eddy-mediated regime transitions in the seasonal cycle of a Hadley circulation and implications for monsoon dynamics. *J. Atmos. Sci.*, **65**, 915–934, doi: 10.1175/2007JAS2415.1.

Schneider, T., and C. C. Walker, 2008: Scaling laws and regime transitions of macroturbulence in dry atmospheres. *J. Atmos. Sci.*, **65**, 2153–2173, doi: 10.1175/2007JAS2616.1.

Shell, K. M., and I. M. Held, 2004: Abrupt transition to strong superrotation in an axisymmetric model of the upper troposphere. *J. Atmos. Sci.*, **61**, 2928–29351, doi: 10.1175/JAS-3312.1.

Walker, C. C., and T. Schneider, 2005: Response of idealized Hadley circulations to seasonally varying heating. *Geophys. Res. Lett.*, **32**, L06813, doi: 10.1029/2004GL022304.

Walker, C. C., and T. Schneider, 2006: Eddy influences on Hadley circulations: Simulations with an idealized GCM. *J. Atmos. Sci.*, **63**, 3333–3350, doi: 10.1175/JAS3821.1.

Xian, P., and R. L. Miller, 2008: Abrupt migration of the ITCZ into the summer hemisphere. *J. Atmos. Sci.*, **65**, 1878–1895, doi: 10.1175/2007JAS2367.1.